HEDL-SA-2183FP

CONF-801107--57

# CONTAMINATION TRANSPORT IN THE PRIMARY COOLANT SYSTEM DURING A BREACHED FUEL PIN TEST IN EBR-II

R.P. Colburn and H.P. Maffei



American Nuclear Society Winter Meeting

Washington, D.C., November 1980

**HANFORD ENGINEERING DEVELOPMENT LABORATORY**
**Operated by Westinghouse Hanford Company, a subsidiary of Westinghouse Electric Corporation, under the Department of Energy Contract No. EY-76-C-14-2170**

---

# CONTAMINATION TRANSPORT IN THE PRIMARY COOLANT SYSTEM DURING A BREACHED FUEL PIN TEST IN EBR-II

R.P. Colburn and H.P. Maffei

A major concern in operating an LMFBR with breached fuel is the potential spread of contamination in the primary coolant system. Such contamination could significantly impact the maintenance of plant components. A deposition sampler experiment was designed to obtain representative specimens of debris which are released from an operating breached fuel pin in EBR-II. A study of these deposits gives a basis to determine the magnitude and nature of the released contamination and provides data to predict the transport and deposition behavior of the contaminants in the primary coolant system. This information is needed to assess the impact of Run Beyond Cladding Breach (RBCB) operation on plant systems.

The first deposition sampler test was performed in the Breached Fuel Test Facility (BFTF) at EBR-II using a naturally breached mixed oxide fuel pin source (XY-2). The source pin breached after about 7 at % burnup and continued to operate at steady power, 41 Kw/m, for 7 days following the breach. The effluent from the XY-2 assembly was directed into the BFTF which contained flowmeters, thermocouples, a delayed neutron detector, and the deposition sampler.

The sampler was located ∿ 1.5 m above the subassembly outlet in a well shielded region above the reactor vessel cover as shown in Figure 1. The sampler details are illustrated schematically in Figure 2. The sodium entering the bottom of the sampler was divided into two concentric flow paths. The outer annular path carried half of the flow (18.9 l/min) across test deposition rings. The rings provided a range of material compositions and surface finishes. The parallel inner flow path guided the remaining flow through a sintered 316 stainless steel cylindrical filter with nominal pore size of 10 μm to retain particulates.

The BFTF containing the sampler was gamma scanned at EBR-II shortly after its removal from the reactor. The scan showed $^{140}$Ba-$^{140}$La was the dominant contaminant with large deposits above (downstream from) the sampler.

Some of these gamma scan data are shown in Table 1. A detailed examination of the sampler was not performed until several months after removal from the reactor after the $^{140}$Ba-La activity had decayed to very low levels. At that time $^{140}$Ba-$^{140}$La was still found mainly on the upper end of the sampler. It was also

found at two lower points; one near the base of the standpipe below the filter and the other near the mid-point of the filter. These two points corresponded to two regions of high concentration of fuel and other fission products and the $^{140}$Ba-La activities in these deposits are believed to be associated with particulates stopped by the filter. However, the $^{140}$Ba-La concentration on the surfaces downstream from the filter were comparable to those in the unfiltered outer annular flow path. This was in striking contrast to the fuel and most other fission product concentrations which were much lower downstream from the filter.

Feuerstein (1) reported enhanced release of $^{140}$Ba and $^{141}$Ce, due to volatile precursors, during breached fuel tests in the SILOE reactor. The transport and deposition behavior of these species in the BFTF can be understood in terms of release both as volatile precursors in solution in the sodium and as species incorporated in particulates.

The $^{140}$Cs ($\tau_{1/2}$ = 65 sec) precursor provides a mechanism which could account for the relatively large concentrations of $^{140}$Ba downstream from the filter. While existing as a Cs isotope precursor it would tend to remain dissolved in the sodium and be transported in the coolant. After decay to barium, rapid deposition on the surfaces would be expected. This type of behavior of barium tracer in sodium has been widely observed in sodium systems containing $^{137}$Cs tracer (2,3,4). In the case of $^{137}$Cs, its $^{137}$Ba ($\tau_{1/2}$ = 2.6 min) daughter emits the characteristic 0.662 MEV gamma which is often associated with $^{137}$Cs. However, in flowing sodium systems, the deposition of $^{137}$Ba on sodium loop surfaces is often so rapid that the local secular equilibrium between $^{137}$Cs and $^{137}$Ba is upset and the 0.662 MEV gamma no longer represents the $^{137}$Cs distribution. M.H. Cooper (4) reported the rate of $^{137}$Ba deposition in his tests could be described by classical liquid state mass transfer. By analogy, we can assume the $^{140}$Ba, born from $^{140}$Cs dissolved in sodium, would similarly deposit on system surfaces with its rate of deposition limited by the mass transport conditions in the coolant stream. The distribution of $^{140}$Ba incorporated in particulates would of course be determined by the transport and deposition of the particals and the overall $^{140}$Ba distribution would be determined by the combination of the two mechanisms.

Similarly, the $^{141}$Ce distribution suggests its transport was determined by both particulate release and the release and decay of the $^{141}$Cs ($\tau_{1/2}$ = 25 sec) precursor. The $^{141}$Cs decays to $^{141}$Ba. Once the $^{141}$Ba isotope has deposited on a surface, it would tend to remain on the surface for subsequent decay to $^{141}$La and $^{141}$Ce.

The $^{141}Ce$ concentrations at various points on the sampler surfaces are shown in Table 2. The large concentrations on the filter are associated with particulates trapped by the filter. The $^{141}Ce$ concentrations on the surfaces downstream from the filter were comparable to those in the unfiltered outer annulus which was in marked contrast with $^{144}Ce$ concentrations which were a factor of 5 lower downstream from the filter. Furthermore, the $^{141}Ce$ concentrations on the outer surface of the containment tube, which reflects deposition from the coolant returning from the upper end of the BFTF, were greater than the concentrations on the deposition rings, which reflects deposition from the sodium before it has entered the upper end of the BFTF. This deposition pattern results from the continuing decay of $^{141}Cs$ in the sodium and subsequent deposition of the resulting $^{141}Ba$.

After decay of the $^{140}Ba$-$^{140}La$ activity, $^{95}Zr$-$^{95}Nb$ was the principal gamma activity remaining in the sampler. Other radionuclides found included $^{141}Ce$, $^{144}Ce$, $^{154}Eu$, $^{103}Ru$, $^{106}Ru$, and $^{54}Mn$. Some $^{137}Cs$ was found at two isolated locations. However, the flowing sodium swept most of it through the sampler leaving only trace amounts of $^{137}Cs$ in the small heel of undrained sodium. Much of the radioactivity was loosely adherent and smearable.

The distributions of some of the more important contaminates among the sampler surfaces are shown in Figures 3, 4, and 5. These figures show the major deposition occurred on the filter. Figure 6 shows a comparison of the relative amounts of the more important contaminants on the filter (decay corrected to reactor shutdown). The figure shows an unusual distribution of contamination on the filter with a large concentration of activity near the middle, with much less activity on the upper end. There were also relatively large concentrations of loose contaminates around the base of the standpipe below the filter, equal to approximately half the contamination on the filter. It is not clear whether this distribution was in place at the end of the RBCB test or whether significant re-distribution of the activity occurred when the sampler was removed from the reactor and sodium drained out from the filter section. This drainage would tend to back flush the filter. The extent of this possible re-distribution will be determined by comparison with future tests where sampler units will be equipped with check valves to prevent drainage of the filter section when they are removed from the sodium pool.

Pu concentration on the surfaces downstream from the filter was small compared to deposition on surfaces in the unfiltered outer annulus. This suggests the filter was effective in retaining the bulk of the Pu contamination on it.

The Uranium to Plutonium ratio in the deposits on the various surfaces was constant and very close to the ratio in the breached fuel pin. This suggests they were released, transported, and deposited together as fuel particulates.

In summary, the release and transport behavior of these contaminants can be interpreted in terms of two basic mechanisms: particulate entrainment and solution of volatile, short-lived precursors. Examination of the sampler indicates that for U, Pu, $^{95}$Zr-Nb, $^{103}$Ru, $^{106}$Ru, $^{144}$Ce, and $^{154}$Eu particulate entrainment was the dominant mechanism in this test. The distributions of $^{141}$Ce and $^{140}$Ba-La deposits indicated both mechanisms were significant in the transport of these species.

The sampler provides a sensitive measure of the magnitude of contamination release from a breached fuel pin and detailed information concerning its nature and transport behavior. A total of five deposition sampler tests are planned in conjunction with the Run Beyond Cladding Breach Program at EBR-II. Intercomparison of the data from these tests will provide a statistical basis which will permit prediction of release and transport behavior trends for contamination from breached fuel in an LMFBR.

REFERENCES:


1. H. Feuerstein and H.H. Stamm, "Release of Fission Products and Fuel From Defected Fuel Pins in Sodium Loops", presented at the Second International Conference on Liquid Metal Technology in Energy Production, April 20-24, 1980, Richland, Washington.

2. J.M. Atwood, et al., Sodium Technology Progress Report, January-March 1978, HEDL-TME-78-90, January, 1979.

3. H.E. Evans and W.R. Watson, "Bahavior of Dilute Solutions of Cesium and Barium in Liquid Sodium", Proc. BNES International Conference Liquid Alkali Metals, Nottingham, U.K., 1973.

4. M.H. Cooper and S.H. Chiang, "Radiochemical Measurement of Mass Transport in Sodium", Proc. International Conference Liquid Metal Technology in Energy Production, Champion, Pennsylvania, 1976.

TABLE I

GAMMA SCAN DATA FROM BFTF CONTAINING THE DEPOSITION SAMPLER

(October 25, 1979)

| Elevation (cm) | Position Description | Counts/min $^{140}Ba$-$^{140}La$ | Counts/min $^{95}Zr$-$^{95}Nb$ |
|---|---|---|---|
| 0 | Bottom of Deposition Sampler | 1,200 | 0 |
| 61 | | 3,700 | 700 |
| 92 | | 20,000 | 1,760 |
| 107 | | 16,300 | 340 |
| 137 | Top of Deposition Sampler | 7,600 | 350 |
| 183 | | 10,600 | 250 |
| 244 | | 19,000 | 150 |
| 274 | Flowmeter | 17,700 | 140 |
| 396 | | 20,400 | Trace |
| 457 | (Flow Turn Around) | 21,800 | 0 |
| 518 | | 770 | 0 |

TABLE 2

$^{141}Ce$ CONCENTRATIONS ON SURFACES OF DEPOSITION SAMPLER

| SURFACE LOCATION | $^{141}Ce$ $\mu Ci/cm^2$ |
|---|---|
| Filter | |
| Bottom | 13.9 |
| 25 cm From Bottom | 28.5 |
| Top Piece | |
| I.D. (Downstream From Filter) | 1.36 |
| O.D. (Top End-Outer Annulus) | 1.29 |
| Outer Casing | |
| I.D. (Upstream From BFTF) | .71 |
| O.D. (Downstream From BFTF) | .81 |

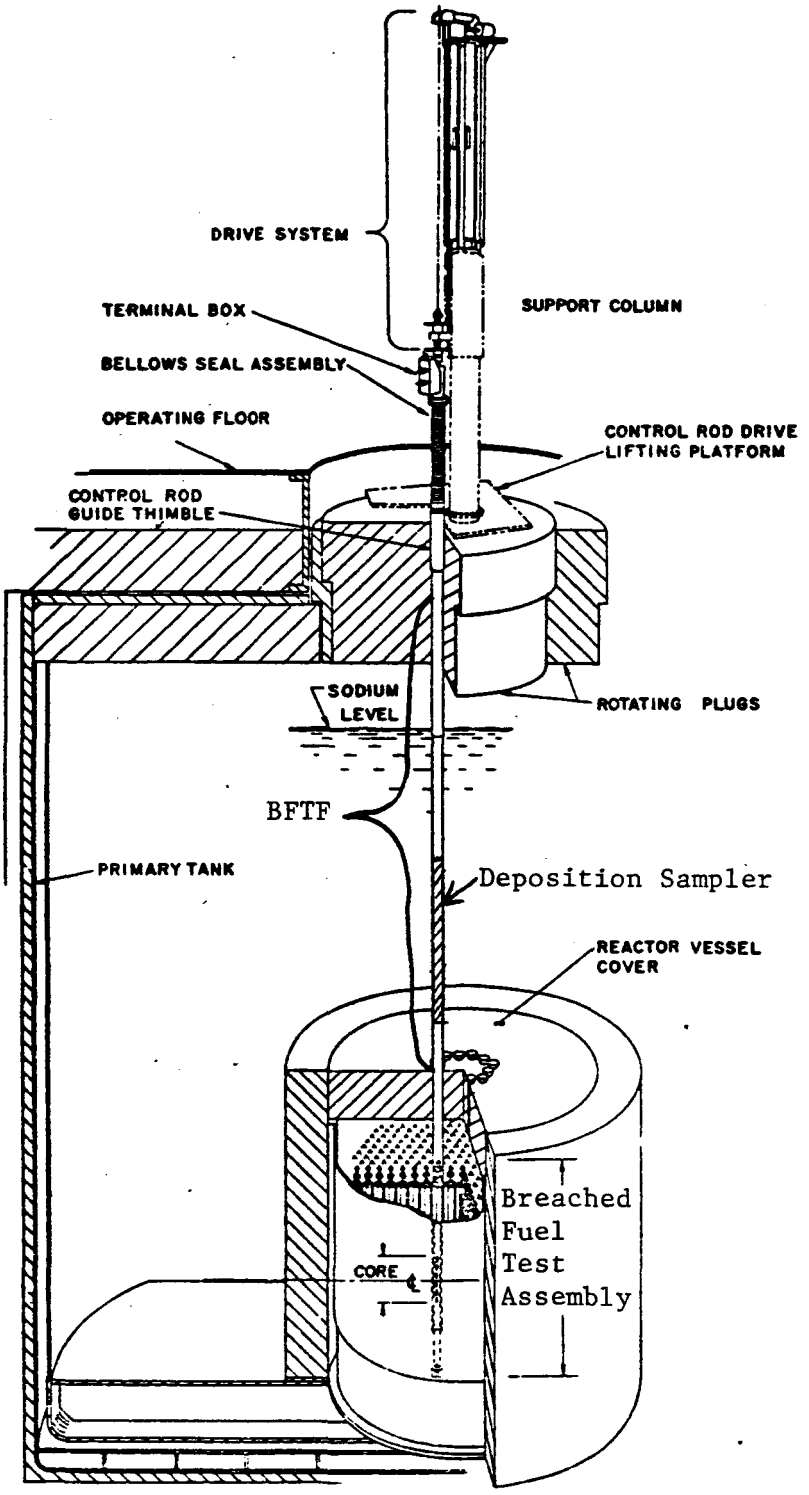
DRIVE SYSTEM
TERMINAL BOX
SUPPORT COLUMN
BELLOWS SEAL ASSEMBLY
OPERATING FLOOR
CONTROL ROD DRIVE
LIFTING PLATFORM
CONTROL ROD
GUIDE THIMBLE
SODIUM
LEVEL
ROTATING PLUGS
BFTF
PRIMARY TANK
Deposition Sampler
REACTOR VESSEL
COVER
Breached
Fuel
Test
Assembly
CORE

FIGURE 1

# DEPOSITION SAMPLER

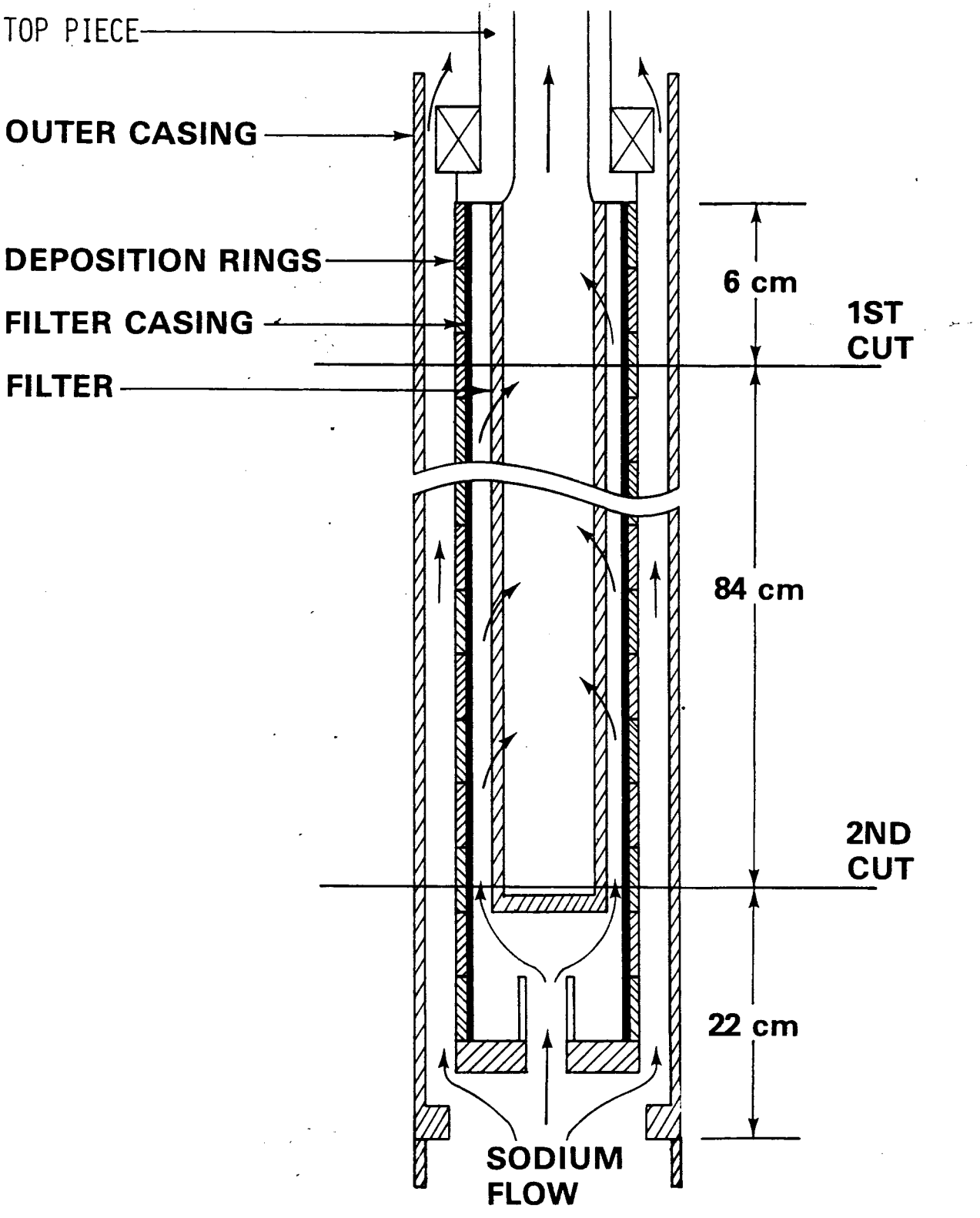


FIGURE 2

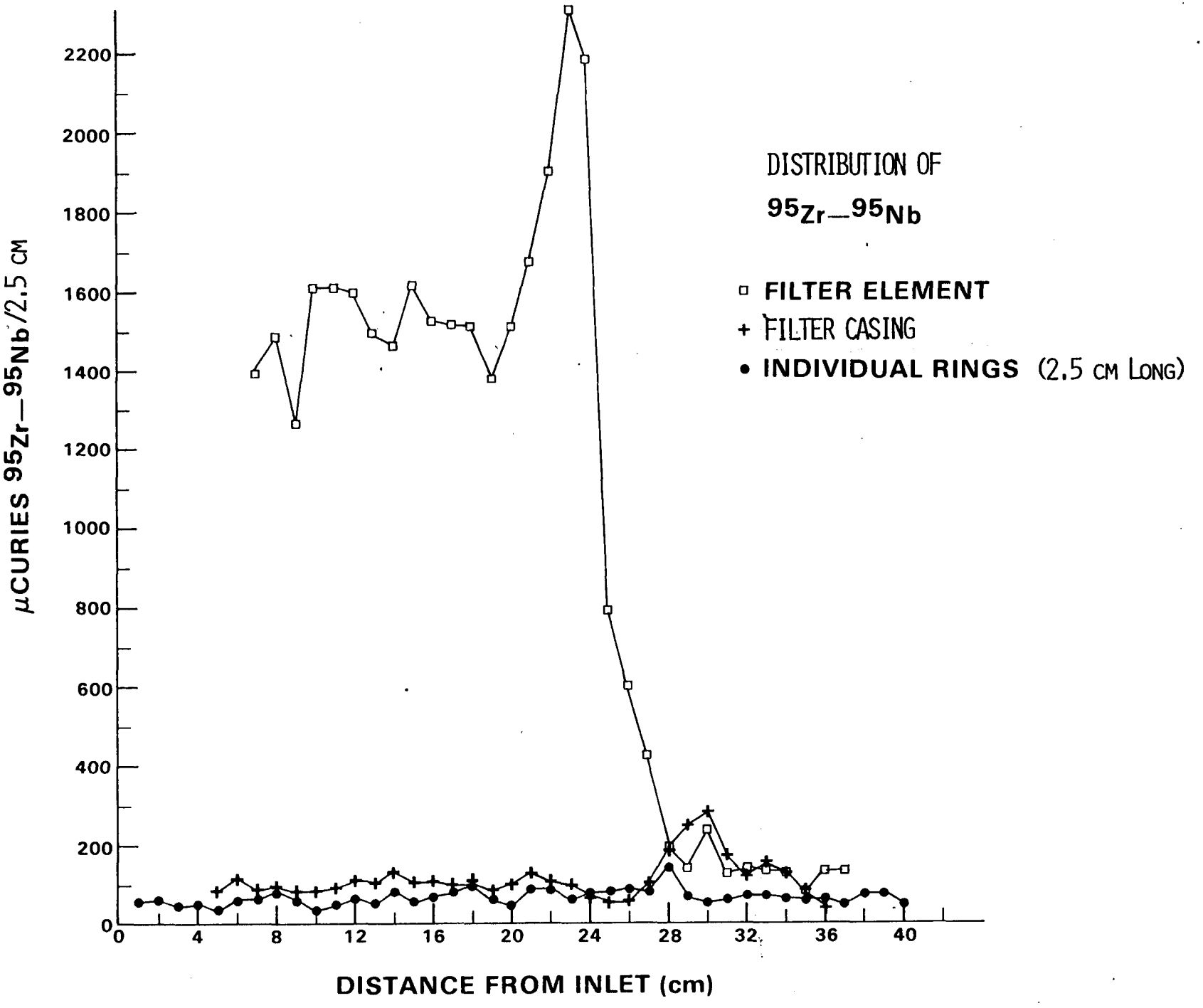
DISTRIBUTION OF
95Zr—95Nb
FILTER ELEMENT
FILTER CASING
INDIVIDUAL RINGS (2.5 CM LONG)
μCURIES 95Zr—95Nb/2.5 CM
DISTANCE FROM INLET (cm)
0
200
400
600
800
1000
1200
1400
1600
1800
2000
2200
0
4
8
12
16
20
24
28
32
36
40

FIGURE 3

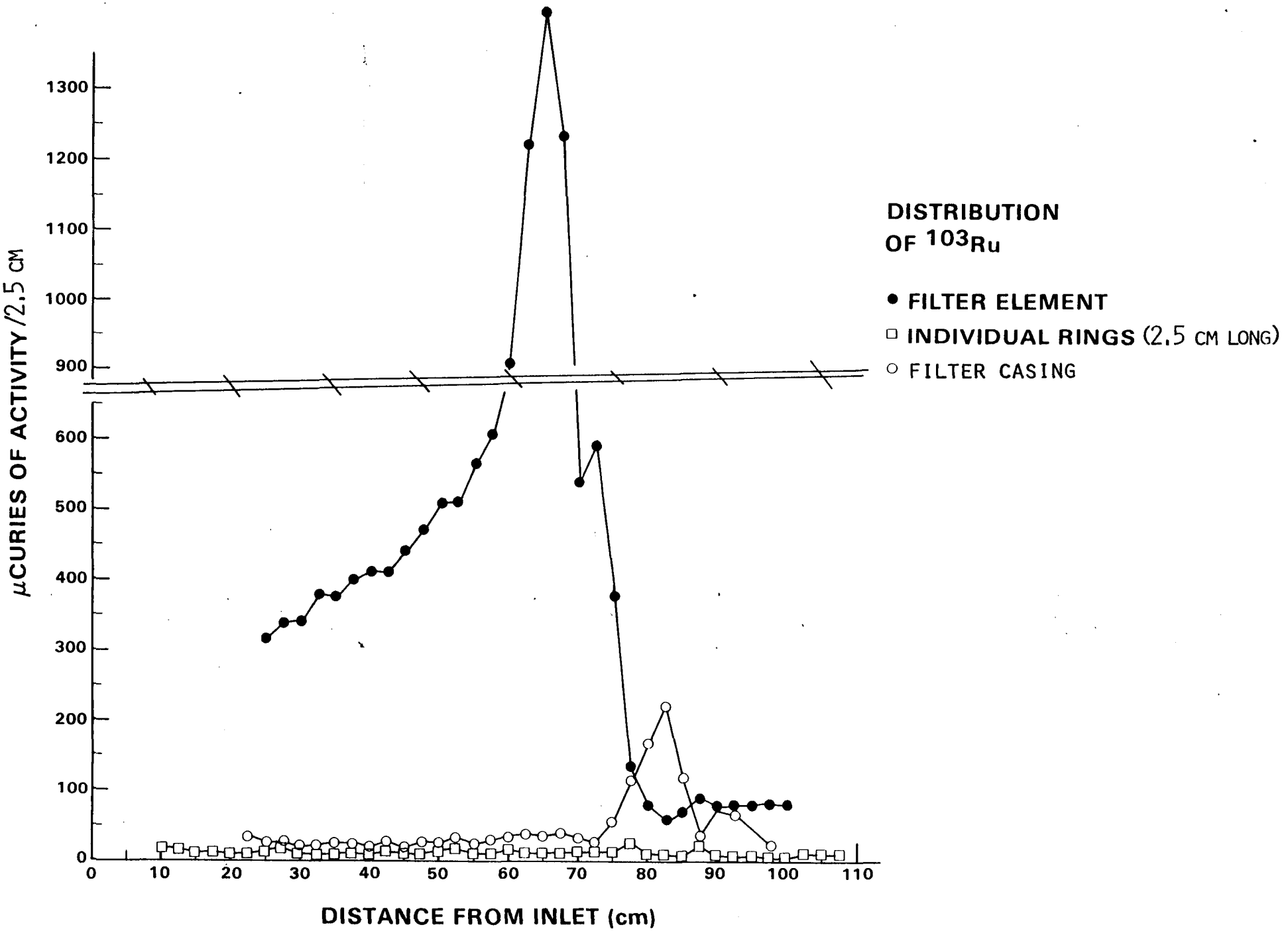
DISTRIBUTION
OF $^{103}Ru$
● FILTER ELEMENT
□ INDIVIDUAL RINGS (2.5 CM LONG)
○ FILTER CASING
μCURIES OF ACTIVITY/2.5 CM
1300
1200
1100
1000
900
600
500
400
300
200
100
0
0
10
20
30
40
50
60
70
80
90
100
110
DISTANCE FROM INLET (cm)

FIGURE 4

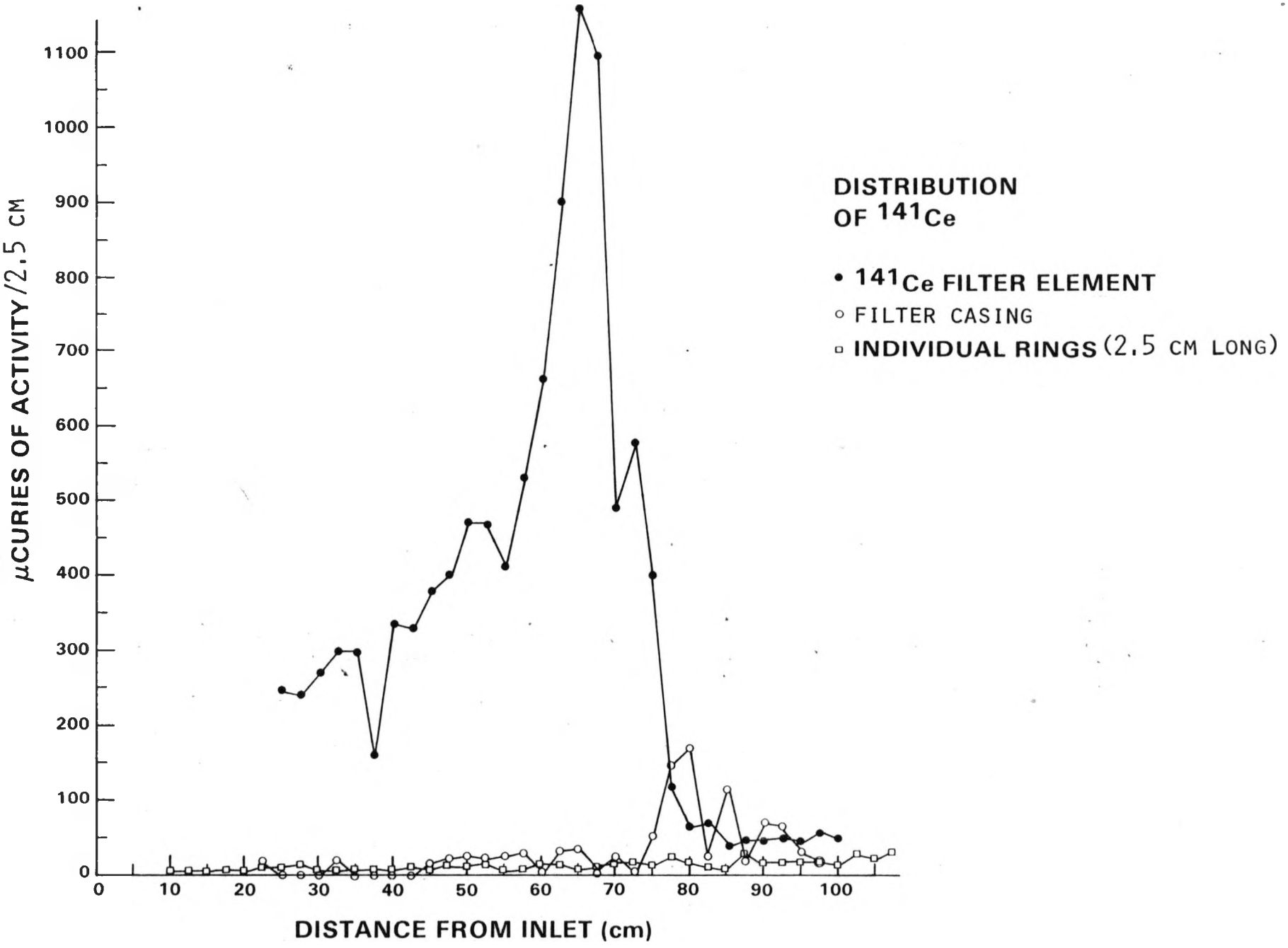
DISTRIBUTION
OF 141Ce
• 141Ce FILTER ELEMENT
○ FILTER CASING
▫ INDIVIDUAL RINGS (2.5 CM LONG)
μCURIES OF ACTIVITY/2.5 CM
0
100
200
300
400
500
600
700
800
900
1000
1100
0
10
20
30
40
50
60
70
80
90
100
DISTANCE FROM INLET (cm)

FIGURE 5

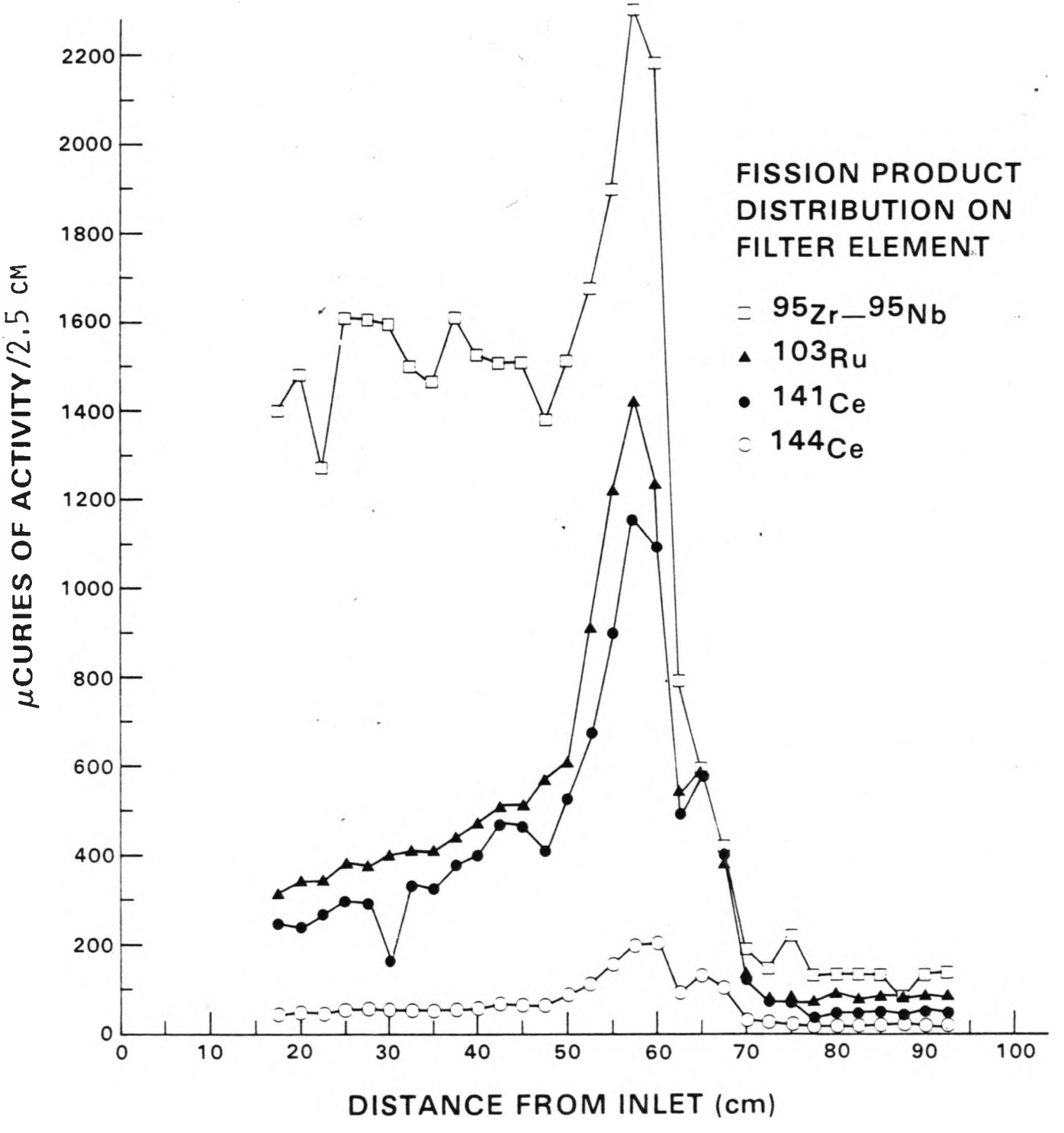


GAMMA SCAN OF DEPOSITION SAMPLER FILTER

FIGURE 6